DOI 10.5162/sensoren2024/D1.1

Ultrasound-based Detection of Objects in Grain Fields

Florian Troendle[1], *Benedikt George*[1], *Florian Hubert*[1, 2] *and Stefan J. Rupitsch*[1]
[1] Laboratory for Electrical Instrumentation and Embedded Systems, Department of Microsystems Engineering - IMTEK, University of Freiburg, Freiburg, Germany
[2] Siemens Healthineers AG, Corporate Testing Laboratory, Erlangen, Germany
florian.troendle@imtek.uni-freiburg.de

Summary: Foreign objects in a crop, such as stones, can cause serious damages if they collide with a grain harvester. Machine damages result in downtimes during the tightly scheduled harvesting phase and lead to additional costs. Currently, there are no technical systems that warn an operator in the case of a collision with foreign objects during harvesting. Therefore, this contribution examines ultrasound-based methods for stone detection. Since ultrasonic sensors are very robust and reliable, these transducers are very common in the agricultural sector. The propagation of acoustic waves within a grain field was examined using a realistic replication. The evaluation criteria during the experiments were the attenuation of the acoustic signal by the crop, the influence of the soil and the arrangement of the ultrasonic sensors. We used mono-frequency, sinusoidal burst sequences with a frequency of 50 kHz and a duty cycle of 0.01 % as acoustic stimulation signals. A synthetic aperture focusing technique was applied to improve the lateral resolution. A vertical alignment of the ultrasonic transducers produced the best possible object resolution.

Keywords: Ultrasonic imaging, object detection, synthetic aperture focusing technique, agriculture, sound propagation

Introduction

Detecting stones in a crop is a challenging task for a grain harvester driver. A stone collision can cause major damages to the harvester. Machine damages result in long down times during the harvesting phase and, thus, in higher harvesting costs. In extreme cases, a stone entering the grain harvester can cause flying sparks, which may lead to a fire in the machine or in the grain field. Therefore, preventive measures must be taken out to reduce the risk of a stone collision damage. In practice, many farmers collect the stones by hand before sowing. However, this measure is labor-intensive. Developing a stone-detection sensor principle offers the potential to increase the operational safety of harvesting machines significantly. Since field work becomes more and more autonomous, sensor technology will become increasingly relevant.

Detecting stones and other foreign objects lying on the farmland face several particular challenges. In addition to severe climatic conditions, such as heat, high dust concentrations, wetness, mechanical stresses caused by shocks and vibrations set high requirements for a stone sensor. A robust sensor system is required that can be used reliably in these different ambient conditions.

Due to their reliability, ultrasonic-based distance sensors have been established in many applications. Sound can propagate undisturbed in almost any environment. Therefore, particles in the air do not affect the functionality of ultrasonic sensors, in contrast to optical sensors. Ultrasonic sensors are also insensitive to contamination, since the sensor's surface cleans itself through vibration. Thanks to these advantages, ultrasound-based sensors are currently applied in systems for navigating a robot between rows of fruit [1] or for measuring moisture in grain silos [2]. The aim of this contribution is to propose a suitable measurement method based on an acoustic sensor principle.

Materials and Methods

Our experimental setup comprises a realistic grain field replica (GFR) (depicted in Fig. 1), a broadband electrostatic ultrasonic transducer (Senscomp 7000, active transducer diameter $\varnothing d_\mathrm{t} = 28,7\,\mathrm{mm}$, center frequency $f_0 = 50\,\mathrm{kHz}$), and a 1/4" Bruel&Kjær measurement microphone (type 4939-A-001) [3, 4]. The investigated GFR consisted of row-wise arranged wheat stalks with a spacing of 120 mm, resulting in a plant density of 800 plants/m^2. Plant spikes reached up to a height $h = 600\,\mathrm{mm}$. Both the transmitter and receiver are mounted on a custom-made 1-D positioning stage above the GFR (see Fig. 5). Our prior investigations have shown that this vertical setup is best suited for the object detection due to the highest signal-to-noise ratio (SNR) observed in echo measurements [5].

A schematic of the complete setup is presented in Fig. 3. To reduce undesired environmental sound interferences and reflections from the propagating sound pulse itself, we placed the setup in an acoustic chamber. As a target object, we utilized a stone with a cross-sectional diameter of approximately $\varnothing d_\mathrm{s} \approx 120\,\mathrm{mm}$.

For the object detection, we scanned the GFR by moving the transducer stepwise ($\Delta x = 2 \cdot 10^{-3}\,\mathrm{m}$) along the x-direction over a total distance of $x = 700\,\mathrm{mm}$ while transmitting

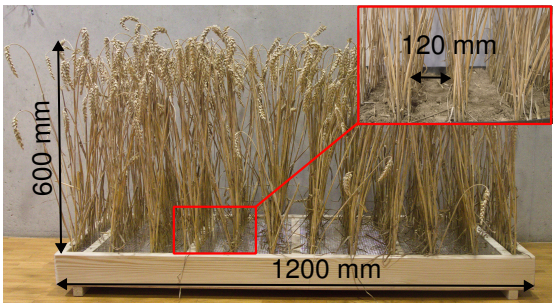

Fig. 1: Replica of the grain field.

sinusoidal burst sequences, each consisting of a 10-cycle, 50 kHz burst with a duty cycle of $D = 0.01\,\%$. Echoes were digitized using an oscilloscope and saved on the computer for subsequent signal processing. The processing procedure involved downsampling of the bandlimited echo, zero-phase bandpass filtering, and calculation of its A-scan, i.e., the echo's envelope obtained through the Hilbert transform. Subsequently, we merged the A-scans to generate a two dimensional, cross-section brightness scan (B-scan) of the GFR (see Fig. 4). Both A-scans and B-scans are popular in medical imaging [6, 7] but have demonstrated utility in our application.

However, as the reflection of the echoes strongly depend on the stone's curvature, the echo's amplitude can be weak leading to a bad SNR and low image quality. Furthermore, the object is located in the positive defocus zone (PDZ) beyond the natural focal plane F, which reads as

$$F = \frac{\varnothing d_\mathrm{t}^2 \cdot f_0}{4 \cdot c} \approx 30\,\mathrm{mm}\,. \qquad (1)$$

On their natural propagation path, the ultrasound pulses pass through the focal area before diverging in a cone under the transducer's pulse-echo beam spread angle (PEBSA) α within the PDZ. As a result, echoes from objects located within the PDZ become distorted, causing crescent-shaped echoes.

To address this challenge, we employed a synthetic aperture focusing technique (SAFT) to enhance the B-scan's lateral image resolution by considering each pixel within the PEBSA. In doing so, the focal area is assumed to be a point acting as a virtual source S. The underlying algorithm is based on the delay-and-sum (DAS) technique, which can be expanded using weighting functions such as Hamming window or Boxcar [8]. The Hamming window is utilized to suppress side lobes, whereas the Boxcar window corresponds to the calculation of a mean [9]. Typically, the weighting approach considers the vertical angle of the transducer relative to the object. Echoes reflected from positions close to the maximum PEBSA underlie weaker weighting compared to echoes reflected on the transducer axis. In contrast, we developed and implemented an *inverse directivity* method to compensate, i.e., invert this angle-dependent weighting approach similar to [10].

We applied the SAFT method to echoes within the transducer's -6 dB PEBSA, which is defined as

$$\alpha_{-6\,\mathrm{dB}} = \arcsin\left(\frac{0.51 \cdot c}{f_0 \cdot \varnothing d_\mathrm{t}}\right) \cdot 2\,, \qquad (2)$$

with the speed of sound in air $c_\mathrm{air} = 343\mathrm{m/s}$, the ultrasound frequency f_0, and the transducer's active diameter $\varnothing d_\mathrm{t}$.

The method's related weighting factor k in the interval $\gamma = [-7^\circ, 7^\circ]$ reads as

$$k(\gamma) = 1 - 1.5660 \cdot \gamma^2 + 0.6205 \cdot \gamma^4\,. \qquad (3)$$

The angle γ indicates the location of the virtual source S to be evaluated relative to the transducer axis.

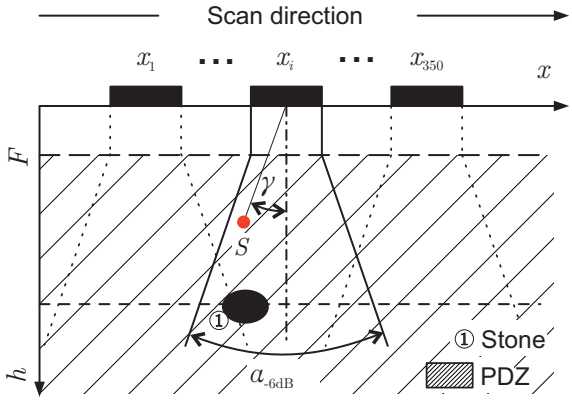

Fig. 2: Geometric representation of the SAFT [7].

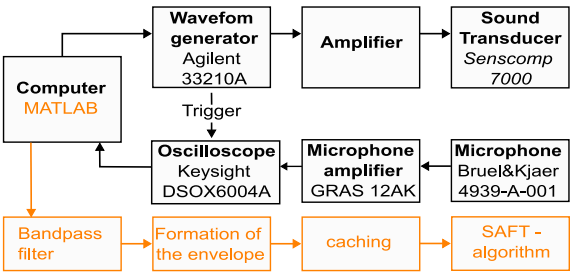

Fig. 3: Schematic representation of the measurement sequence and processing of the data.

Results

The B-scan of our vertical pulse-echo approach is depicted in Fig. 4. The conventional B-scan, as shown in Fig. 4, exhibits speckles in the upper image cluster c_1 (interval $x = [0; 700]$ mm and $h = [400; 600]$ mm), which are caused by the spikes of the plants. A second cluster can be identified in cluster c_2 (interval $x = [0; 700]$ mm and $h \approx 0$ mm), which captures the reflections

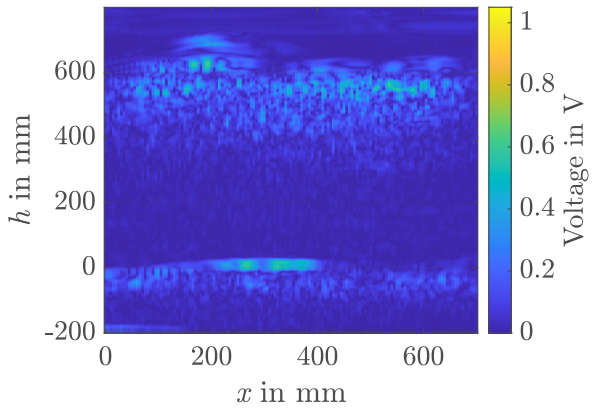

Fig. 4: B-Scan of the grain field with echoes from grain spikes, ground, and stone.

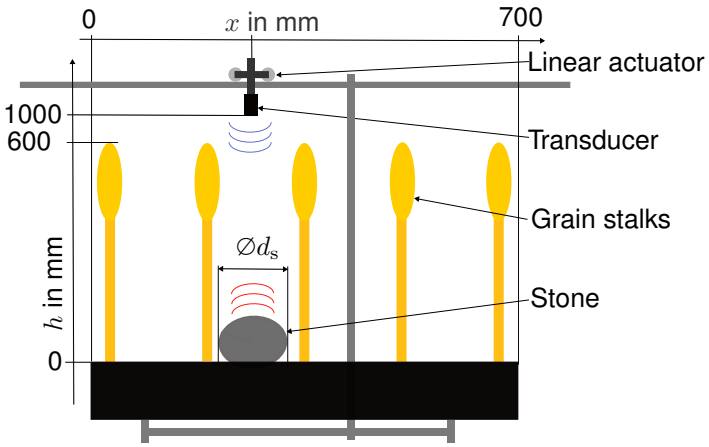

Fig. 5: Schematic representation of the vertical pulse-echo setup, with transmitted pulses illustrated in blue and echoes highlighted in red.

from the ground of the GFR. Additionally, a third cluster c_3 (interval $x = [200; 420]$ mm and $h = [0; 100]$ mm) highlights the stone within the GFR. The stone's crescent-shaped echo can be clearly seen.

Given that the conventional B-scan failed to satisfactorily identify the stone, we post-processed the B-scan using the SAFT algorithm, employing the three weighting methods (see Fig. 6). For comparison, Fig. 6 (a) presents the dB-scaled B-scan in addition. Fig. 6 (b) illustrates the B-scan post-processed using the Boxcar method, which notably enhances the lateral resolution (in the x-direction), emphasizing the contrast of the stone's edge profile. By applying the Hamming weighting, we succeeded in reducing the speckles; however, it also caused blurring of the stone echo [see Fig. 6 (c)]. Conversely, the *inverse directivity* method accentuated the echoes of the stone compared to the surrounding area, resulting in the best image contrast and enhancing the likelihood of stone detection. Although the stone's edge profile hardly improved with this method, it remains relevant for detecting objects where accurately capturing shape is of secondary importance.

Discussion and Summary

This contribution introduced an ultrasound-based method for detection of foreign objects in a grain field. A SAFT algorithm was exploited for two-dimensional imaging, which improved the lateral resolution. For the experimental verification, a realistic replicate of a grain field was used. A vertical pulse-echo arrangement could provide a sensitivity improvement due to the shorter distance traveled in the grain crop. The attenuation of the grain stalks and the selection of an appropriate weighting function for the signal processing were the main challenges concerning the object detection. In our measurements, all test objects were successfully detected.

Our future work will concentrate on a practical verification of the proposed detection concept. For example, measurements during the harvesting phase should clarify in which extent noise and vibrations of the harvester have a cross-influence on our object detection algorithm.

In addition to object detection, the data obtained can also be used to measure the ground contour. This can enable improved height control of the cutterbar. Furthermore, the density of the ears per square meter can be derived from the scans and, thus, the corn yield can be predicted. This enables an optimization of the harvester's forward speed. Therefore, our future research will also go towards this direction.

References

[1] N. M. Thamrin et al. "Tree detection profile using a single non-intrusive ultrasonic sensor for inter-row tracking application in agriculture field". In: *2013 IEEE 9th International Colloquium on Signal Processing and its Applications (CSPA 2013)*. Piscataway, NJ, 2013, pp. 310–313. DOI: 10.1109/CSPA.2013.6530063.

[2] Anchen Shao and Jian Chu. "Design and Research of an Ultrasonic Grain Moisture Content Detection Device". In: *2021 IEEE 4th Advanced Information Management, Communicates, Electronic and Automation Control Conference (IMCEC)*. 2021, pp. 692–696. DOI: 10.1109/IMCEC51613.2021.9482332.

[3] SensComp Inc. *Series 7000 Ultrasonic Sensor Datasheet*. 2022.

[4] Bruel&Kjaer. *1/4-inch Free-Field Microphone Type 4939 Datasheet*. 2021.

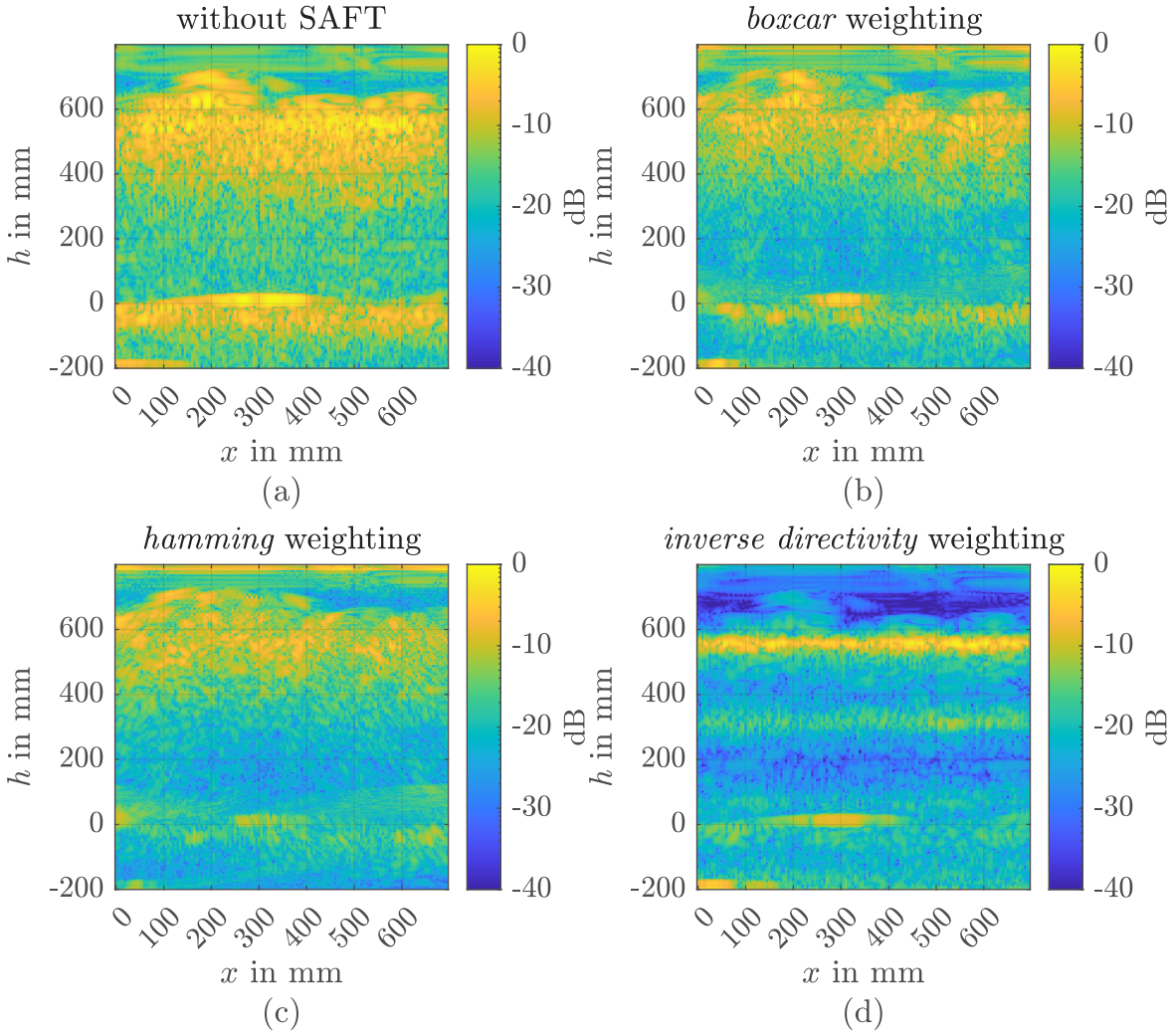

Fig. 6: (a) Conventional B-scan of the grain field and (b)-(d) post-processed B-scans by applying the SAFT algorithm using several weighting methods.

[5] Florian Tröndle. “Evaluation eines geeigneten akustischen Messverfahrens zur Erkennung von Fremdkörpern in einem erntereifen Getreidebestand”. Bachelor Thesis (Supervisors: Benedikt George, Stefan J. Rupitsch). IMTEK Uni Freiburg, 2023.

[6] Stefan J. Rupitsch. *Piezoelectric Sensors and Actuators*. Berlin: Springer, 2019.

[7] Michael Wüst, Johannes Eisenhart, Michael Nierla, Stefan J. Rupitsch. “Simulationsgestütze synthetische Aperaturfokussierungstechnik für die Anwendung in der Ultraschalmikroskopie”. In: *DAGA 2018 München* (2018).

[8] Stefan J. Rupitsch and Bernhard G. Zagar. “Acoustic Microscopy Technique to Precisely Locate Layer Delamination”. In: *IEEE Transactions on Instrumentation and Measurement* 56.4 (2007), pp. 1429–1434. DOI: 10.1109/TIM.2007.899866.

[9] C.H. Frazier and W.D. O’Brien. “Synthetic aperture techniques with a virtual source element”. In: *IEEE Transactions on Ultrasonics, Ferroelectrics, and Frequency Control* 45.1 (1998), pp. 196–207. DOI: 10.1109/58.646925.

[10] Stefan J. Rupitsch and Bernhard G. Zagar. “Verfahren zur Erhöhung der örtlichen Auflösung bei synthetisch fokussierten Ultraschalltransducern (A Method to Increase the Spatial Resolution of Synthetically Focussed Ultrasound Transducers)”. In: *tm - Technisches Messen* 75.4 (2008), pp. 259–267. DOI: 10.1524/teme.2008.0836.